Stable higher-order vortices and quasivortices in the discrete nonlinear Schrödinger equation

P. G. Kevrekidis,[1] Boris A. Malomed,[2] Zhigang Chen,[3] and D. J. Frantzeskakis[4]
[1]*Department of Mathematics and Statistics, University of Massachusetts, Amherst, Massachusetts 01003-4515, USA*
[2]*Department of Interdisciplinary Studies, Faculty of Engineering, Tel Aviv University, Tel Aviv 69978, Israel*
[3]*Department of Physics and Astronomy, San Francisco State University, California 94132, USA and TEDA College, Nankai University, Tianjin, 300457, People's Republic of China*
[4]*Department of Physics, University of Athens, Panepistimiopolis, Zografos, Athens 15784, Greece*
(Received 7 December 2003; revised manuscript received 20 April 2004; published 18 November 2004)

Vortex solitons with the topological charge $S=3$, and "quasivortex" (multipole) solitons, which exist instead of the vortices with $S=2$ and 4, are constructed on a square lattice in the discrete nonlinear Schrödinger equation (true vortices with $S=2$ were known before, but they are unstable). For each type of solitary wave, its stability interval is found, in terms of the intersite coupling constant. The interval shrinks with increase of S. At couplings above a critical value, oscillatory instabilities set in, resulting in breakup of the vortex or quasivortex into lattice solitons with a lower vorticity. Such localized states may be observed in optical guiding structures, and in Bose-Einstein condensates loaded into optical lattices.

DOI: 10.1103/PhysRevE.70.056612 PACS number(s): 42.65.Tg, 52.35.Mw, 03.75.−b

I. INTRODUCTION

In the last two decades, intrinsic localized modes in nonlinear dynamical lattices (known as *discrete breathers*) have become a topic of intense theoretical and experimental investigation, due to their inherent ability to concentrate and (potentially) transport energy in a coherent fashion; for recent reviews of the topic, see Refs. [1]. Settings in which these entities, strongly localized on the lattice and periodic in time, are important collective excitations range from arrays of nonlinear-optical waveguides [2] to Bose-Einstein condensates (BECs) in periodic potentials [3], and from various models based on nonlinear springs [4] to Josephson-junction ladders [5] and dynamical models of the DNA double strand [6].

One of the most ubiquitous (and, simultaneously, most convenient for analysis) models in which such modes have been extensively studied is the discrete nonlinear Schrödinger (DNLS) equation [7]. Its most straightforward physical realization was found in one-dimensional (1D) arrays of coupled optical waveguides [8,9]. Such arrays may be multicore structures made in a slab of a semiconductor material (AlGaAs) [9] or silica [10], or virtual ones, induced by a set of laser beams illuminating a photorefractive crystal [11]. In this experimental implementation of the DNLS system, the number of lattice sites (guiding cores) is $\simeq 40$, and the available propagation distance is up to 20 diffraction lengths of the localized mode, which lends enough room to create discrete solitons and conduct various experiments with them, including collisions [12]. Very recently, discrete diffraction of light was demonstrated experimentally in a bundle of optical waveguides with a regular 2D square-lattice transverse structure, of size up to 7×7, made in fused silica [13]. Actually, lattices of a much larger size, such as 112×112, can be readily created in a photorefractive crystal, with amplitude modulation of a partially coherent beam.

An array of BEC droplets trapped in a strong optical lattice (OL), with $\sim 10^3$ atoms in each droplet, is another direct physical realization of the DNLS equation [3]. In this case, it can be systematically derived via a Wannier-function decomposition [14].

Recently, the idea of light-induced photonic lattices has emerged in nonlinear optics [15] (it is the basis for the above-mentioned virtual lattices used in the experiments with photorefractive media [11]). It arises from the possibility of modifying the refractive index of a nonlinear medium by means of a periodic pattern of intensity modulation, created by a grid of strong beams, while a weaker beam (which, however, experiences much stronger nonlinearity) is used to probe the resulting structures. Promising experimental studies of discrete solitons in 1D and 2D lattices were stimulated by this idea [11,16–19].

Theoretical studies have predicted various types of stable discrete solitons that may occur in 1D dynamical lattices, such as twisted solitons and multipulse bound states [20], compactons [21], and gap solitons [22]. The above-mentioned recent advancements in experiments strongly suggest extending the analysis of DNLS solitons to the 2D case. Strictly speaking, photonic lattices in photorefractive materials have different, i.e., saturable, nonlinearity; however, the same robust structures persist (see below). Furthermore the bundled waveguide arrays, reported in Ref. [13], as well as BECs loaded into a 2D optical lattice, can be described by the 2D DNLS model. In particular, of special interest are discrete 2D solitons carrying a topological charge, i.e., *discrete vortices*. In the context of the DNLS equation, the fundamental vortices, with topological charge ("spin") $S=1$, were systematically investigated in Ref. [23], as 2D counterparts of the 1D discrete twisted solitons of [20], the most important issue being their stability. Bound states of 2D DNLS solitons, including both vortex and zero-vorticity ones, were investigated in Ref. [24]. In the context of other 2D lattice models, vorticity-carrying configurations were earlier considered in [25]. Very recently, discrete vortices were observed (and their robustness was demonstrated) in two independent direct experiments in a photonic lattice created in a photorefractive material [26,27].

Similar vortex states were found in a *continuum* model based on the 2D Gross-Pitaevskii equation including a square-lattice periodic potential, which describes a BEC with attractive interparticle interactions (negative scattering length) loaded in the corresponding square OL [28]. Analogous solutions were found in the context of a 2D phenomenological model of photonic crystals [29] as well. In fact, stable vortex solitons can be found in these models also with hexagonal, triangular, or quasiperiodic (rather than square) OLs, and even in the case when the intrinsic interaction is repulsive [30] (in the latter case, the localized structure is of the gap-soliton type).

While it was possible to demonstrate that the fundamental ($S=1$) vortex solitons are stable in all the above-mentioned settings, a challenging issue concerns the stability of higher-order vortices, with $S \geqslant 2$. In the case of the DNLS, a family of $S=2$ vortices was constructed in Ref. [23]; however, they were found to be unstable. The same inference was reported in Ref. [28] for a model based on the Gross-Pitaevskii equation with the square OL. To the best of our knowledge, no example of stable vortices with $S \geqslant 2$ has been reported thus far, either in simulations or in experiment.

On the other hand, similar issues were recently investigated in *uniform* continuum models (ones without an external potential) and cubic-quintic or $\chi^{(2)}:\chi^{(3)}_{-}$ (quadratic–self-defocusing-cubic) nonlinearities. Originally, it was found that only vortex solitons with $S=1$ and $S=2$ were stable in the cubic-quintic model, while the ones with $S \geqslant 3$ were supposed to be unstable [31]. However, it was then demonstrated that the higher-order vortices may be stable too (at least, up to $S=5$), but in very narrow regions [32]. For instance, for $S=3$ solitons the stability domain occupies $\simeq 3\%$ of the existence region (and still less for $S>3$), while for the fundamental ($S=1$) vortices it was $\simeq 10\%$. Very recently, similar results were also obtained for the vortex solitons in the $\chi^{(2)}:\chi^{(3)}_{-}$ model [33]; hence narrow stability domains of higher-order vortex solitons are a generic feature of continuum spatially uniform models with competing nonlinear interactions.

It is relevant to mention that the stable higher-order vortex soliton beams in bulk media may be promising, in applications to photonics, as "light conduits" to guide weak optical signals, since they are "more hollow" than the beams with $S=1$. On the other hand, if, for instance, the vortex beam with $S=2$ is unstable against splitting into two fundamental vortices with $S=1$, which is quite a typical case [31], this may be used to create a Y-shaped ramification of the conduit.

In this work, we address the stability of higher-order vortex solitons in the 2D DNLS model. In particular, this is motivated by the above-mentioned recent experimental demonstration of stable fundamental quasidiscrete vortex solitons [26], and the availability of phase masks which can lend vorticity $S \geqslant 2$ to a laser beam. Experimental search for such higher-order vortex spatial solitons in a photorefractive lattice is currently under way [34]. Here, we demonstrate, by means of accurate numerical calculation of eigenvalues of the linearization around such solitons, that they are *stable* in properly chosen parameter regions of the DNLS model.

The paper is organized as follows. The model is formulated in Sec. II, which also briefly describes numerical techniques employed for the analysis of solutions and their stability. Detailed results for the vortices with $S=3$, whose topological charge (vorticity) can be identified unambiguously through their phase, as the solutions are complex, are presented in Sec. III. The analysis is based on the computation of the full set of corresponding stability eigenvalues. The evolution of unstable solitons is investigated by dint of direct simulations (they split into a set of two stable solitons, with $S=1$ and $S=0$). In Sec. IV we consider solutions that are supposed to play the role of vortices with $S=2$; their counterparts corresponding to $S=4$ are briefly considered too. Unlike true complex vortex solutions with $S=2$, which are known to always be unstable [23], these solutions are purely real ones, having the form of quadrupoles (in the case corresponding to $S=2$). Their vorticity can be directly identified only if a small perturbation, which makes them complex, is added. To this end, we employ the localized eigenmodes of small perturbations around the solutions, and conclude that their vorticity, defined in this fashion, is not 2, but zero. Nevertheless, these localized solutions are qualitatively different from the ordinary $S=0$ solitons; we call them *quasivortices*. The stability region is found for the quasivortices corresponding to both $S=2$ and $S=4$. In an optical experiment, the quasivortices can be created, passing the laser beam through a phase mask, in the same way as for regular vortices.

II. THE MODEL

The DNLS equation on a square lattice has the well-known form [7],

$$i\frac{d}{dt}\phi_{m,n} + C\Delta_2\phi_{m,n} + |\phi_{m,n}|^2\phi_{m,n} = 0, \tag{1}$$

where C is the coupling constant, and Δ_2 stands for the discrete Laplacian, $\Delta_2\phi_{m,n} = \phi_{m+1,n} + \phi_{m,n+1} + \phi_{m,n-1} + \phi_{m-1,n} - 4\phi_{m,n}$. Looking for stationary solutions of the form $\phi_{m,n} = \exp(i\Lambda t)u_{m,n}$, Eq. (1) leads to the time-independent equation

$$\Lambda u_{m,n} = C\Delta_2 u_{m,n} + |u_{m,n}|^2 u_{m,n}. \tag{2}$$

Numerical solutions to Eq. (2) were obtained by means of a Newton method (note that we are interested, generally speaking, in complex solutions, therefore $u_{m,n}$ was decomposed into its real and imaginary parts).

Upon generating stationary solutions, their stability was examined through linearization. To this aim, a perturbed expression of the form [35]

$$\phi_{m,n} = \exp(i\Lambda t)u_{m,n} + \epsilon\exp(i\Lambda t)[a_{m,n}\exp(-i\omega t) + b_{m,n}\exp(i\omega^* t)] \tag{3}$$

was substituted into Eq. (1). Here $u_{m,n}$ is the unperturbed stationary solution, ϵ is an infinitesimal amplitude of the perturbation, and ω is its eigenfrequency (which is imaginary or complex in the case of instability). This leads to the following linear equation for the perturbation eigenmode:

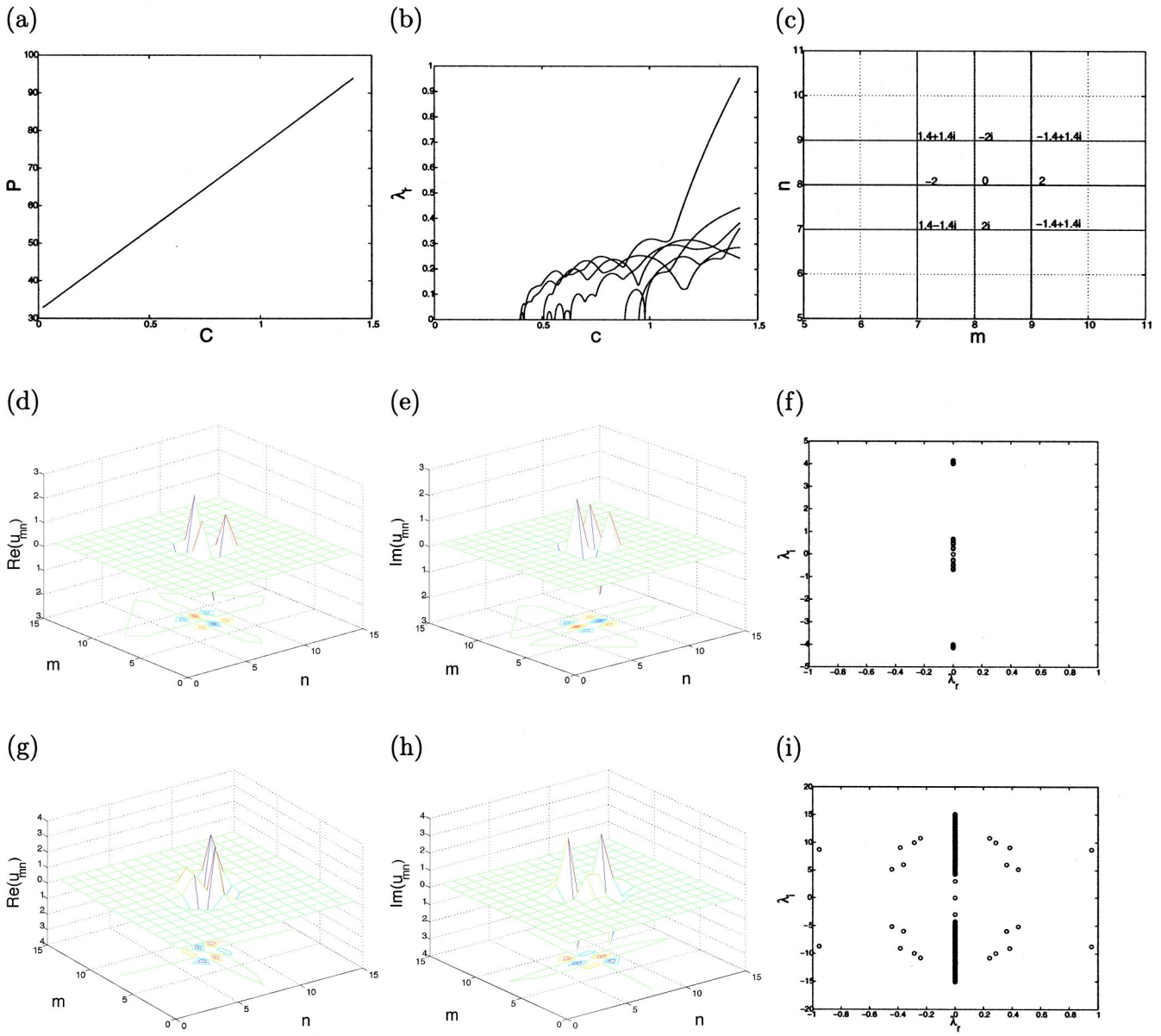

FIG. 1. (Color online) The top left panel shows the norm of the vortex-soliton solution with $S=3$ vs the lattice-coupling strength C. The eigenvalues with the largest real part are shown as a function of C in the top middle panel (instability takes place at $C>0.862$). The top right panel shows a schematic of the two-dimensional structure of the $S=3$ vortex. The approximate complex values of the field $u_{m,n}$ are given for the main sites. Examples of the real and imaginary parts of the profile of the stationary solution and of its spectral plane of stability eigenvalues around it are shown in the left, middle, and right panels (respectively): in the middle row for $C=0.02$ (a stable vortex), and in the bottom row for $C=1.418$ (a strongly unstable one). Note that in the latter case there are eigenvalue quartets accounting for the instability.

$$\omega\begin{pmatrix} a_k \\ b_k^\star \end{pmatrix} = \mathbf{J}\begin{pmatrix} a_k \\ b_k^\star \end{pmatrix}, \tag{4}$$

where $\mathbf{J}$ is the Jacobian matrix

$$\mathbf{J} = \begin{pmatrix} \partial F_k/\partial u_j & \partial F_k/\partial u_j^* \\ -\partial F_k^*/\partial u_j & -\partial F_k^*/\partial u_j^* \end{pmatrix}$$

and $F_i \equiv -C(u_{i+1}+u_{i-1}+u_{i+N}+u_{i-N}-4u_i)+\Lambda u_i - u_i^2 u_i^*$; the string index $k=m+(n-1)N$ maps the $N\times N$ lattice into a vector of length N^2 (indices i and j also take values from the same vector). Numerical solutions were sought for with Dirichlet boundary conditions at the domain boundaries, i.e., at $n=1$, $n=N$ and $m=1$, $m=N$.

We use the obvious scaling invariance of the equation, fixing the frequency $\Lambda=4$ and varying the coupling parameter C, to examine continuous branches of the solutions. In this way, we can cover the whole manifold of discrete-soliton solutions, if their integer vorticity S is varied too. It is relevant to mention that, for the chosen value of $\Lambda=4$, the $S=0$ discrete solitons and $S=1$ fundamental vortices in the DNLS equation are stable in the regions, respectively [23],

$$C \leqslant C_{\rm cr}^{(0)} = 4.0,\ C \leqslant C_{\rm cr}^{(1)} = 1.6. \tag{5}$$

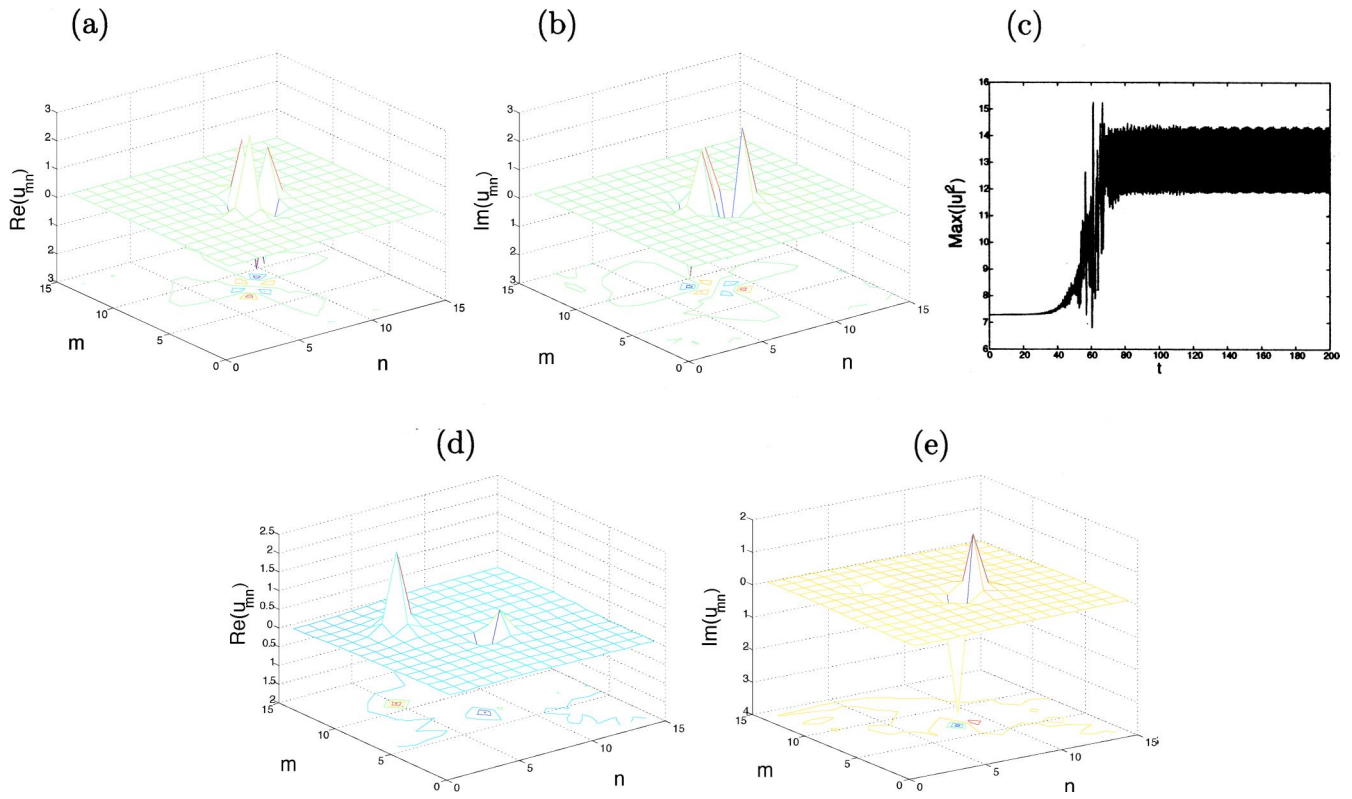

FIG. 2. (Color online) Panels (a) and (b) show the initial unstable $S=3$ vortex for $C=0.618$. The top right panel shows the development of the oscillatory instability in the evolution of the lattice field. The bottom panels show the real and imaginary parts of the eventually established field configuration, which contains stable solitons with $S=0$ and $S=1$.

To generate vortex solutions with given integer S, we initialize the Newton method with a quasicontinuum complex ansatz

$$u_{m,n}^{(\mathrm{init})} = A[(m-m_0)+i(n-n_0)]^S \times \mathrm{sech}(\eta\sqrt{(m-m_0)^2+(n-n_0)^2}), \tag{6}$$

where (n_0, m_0) is the location of the vortex center, and η is its intrinsic scale parameter. To generate numerically exact stationary solutions, the Newton algorithm was iterated until the convergence no worse than 1 part in 10^8 was achieved. After that, a linear stability analysis of the stationary solutions was performed. The results are typically shown for 15×15 site lattices, but it was verified that they do not change for larger sizes.

III. VORTICES WITH $S=3$

Motivated by the presence of stable higher-order vortex solitons in the uniform continuum models [32,33], we started by seeking for $S=3$ solutions in the 2D DNLS equation. Basic results for these vortices are summarized in Fig. 1. The top left panel of the figure displays the norm of the solution, $P=\Sigma_{m,n}|u_{m,n}|^2$ (which has the meaning of the total power of the trapped light beam in the optical waveguide array, or the number of atoms in the trapped BEC) as a function of C, for fixed $\Lambda=4$. Note that, in the quasicontinuum approximation, which corresponds to $C\gg\Lambda$, the dependence $P(C)$ must be linear for a 2D soliton of any type; it is interesting that the linear dependence persists for smaller coupling values.

The instability growth rate of the vortex soliton, i.e., the real part of the most unstable perturbation eigenvalues $\lambda \equiv i\omega$, is shown, as a function of C, in the top middle panel of Fig. 1. The top right panel shows the configuration schematically illustrating the main sites constituting the vortex and (for $C=0.02$) the approximate field values at each one of them. The $S=3$ structure can be clearly discerned from the phase variation which follows an $e^{3i\theta}$ pattern along the lattice. The $S=3$ vortices are stable in the region:

$$C \leqslant C_{\mathrm{cr}}^{(3)} = 0.398, \tag{7}$$

where $\mathrm{Re}\lambda \equiv 0$ [cf. the stability intervals (5) for $S=0$ and $S=1$ solitons]. At the point $C=C_{\mathrm{cr}}^{(2)}$, an instability sets in through a *Hamiltonian Hopf bifurcation* [36], i.e., collision of two real eigenvalue pairs with opposite *Krein signatures* (as was discussed in a general form in Refs. [37,38]). This bifurcation makes the quartet of eigenvalues complex. With subsequent increase of C, we obtain additional destabilizing bifurcations at $C=0.402$, $C=0.508$, $C=0.524$, $C=0.886$, and $C=0.952$, which increase the number of unstable eigenfrequencies. This eventually results in six quartets of unstable eigenvalues for $C=1.418$, as shown in the bottom panel of Fig. 1. Examples of the stationary vortex and spectral plane of its stability eigenvalues (showing their real and imaginary parts λ_r and λ_i), are displayed for a stable case, with C

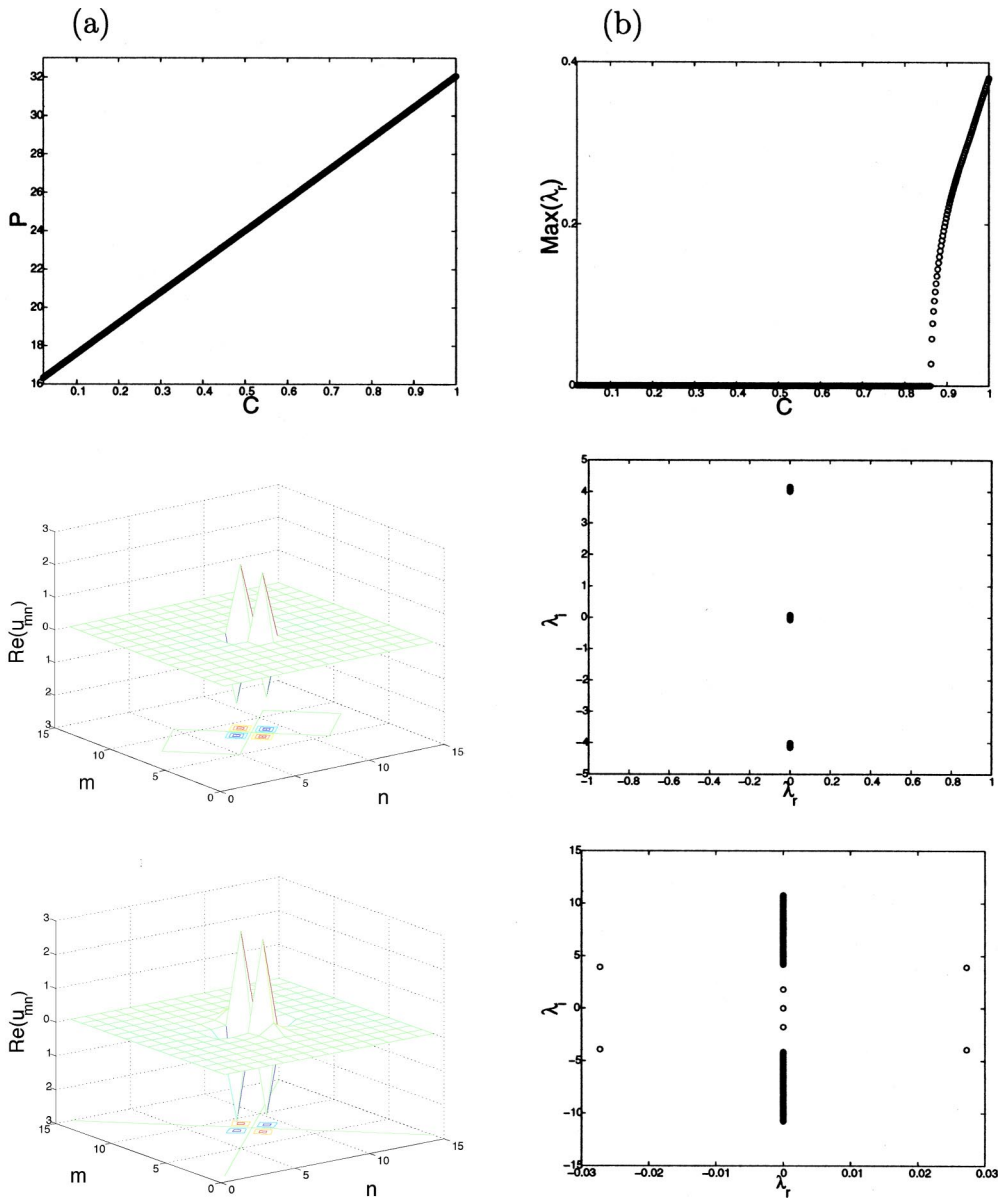

FIG. 3. (Color online) The top left panel shows the norm of the quasivortex solution, corresponding to $S=2$, vs the coupling constant C. The largest real part of the stability eigenvalues is shown as a function of C in the top right panel (instability sets in at $C=0.862$). The (purely real) profile of the stationary solution, and the spectral plane of the associated stability eigenvalues are shown in the left and right panels: in the middle row for $C=0.02$, and in the bottom one for $C=0.862$.

$=0.02$, in the middle panel, and at the instability onset ($C=0.862$) in the bottom panel of Fig. 1.

Nonlinear development of the instability of the $S=3$ vortex in the region $C>0.398$ was examined in a number of cases by means of direct simulations of Eq. (1), using the fourth-order Runge-Kutta method; the instability was initiated by adding a small initial perturbation to the solution. A typical example is shown in Fig. 2 for the case of $C=0.618$. In this case, the original $S=3$ vortex splits into one with $S=1$, which stays at the initial position, and an additional fragment with $S=0$, which separates and eventually gets trapped at a different lattice site. Both the $S=1$ and $S=0$ solitons, generated by the instability from the $S=3$ vortex, are stable at the corresponding values of the parameters. We stress that the apparent nonconservation of the topological charge observed in these simulations is quite possible, as the lattice does not conserve angular momentum.

IV. QUASIVORTICES

The stationary equation (2) admits real solutions. These are generated by the real part of the ansatz (6) with $S=2$ and $S=4$. First, we focus on the presentation of their shape and dynamical properties; then, we will discuss interpretation of such real solutions in terms of vorticity.

For $S=2$, typical results are shown in Figs. 3 and 4. Similar to Fig. 1, the top left and right panels in Fig. 3 show, respectively, the norm of the solution and the instability growth rate as a function of C. As in the case of the $S=3$ vortex, the instability sets in through the Hamiltonian Hopf

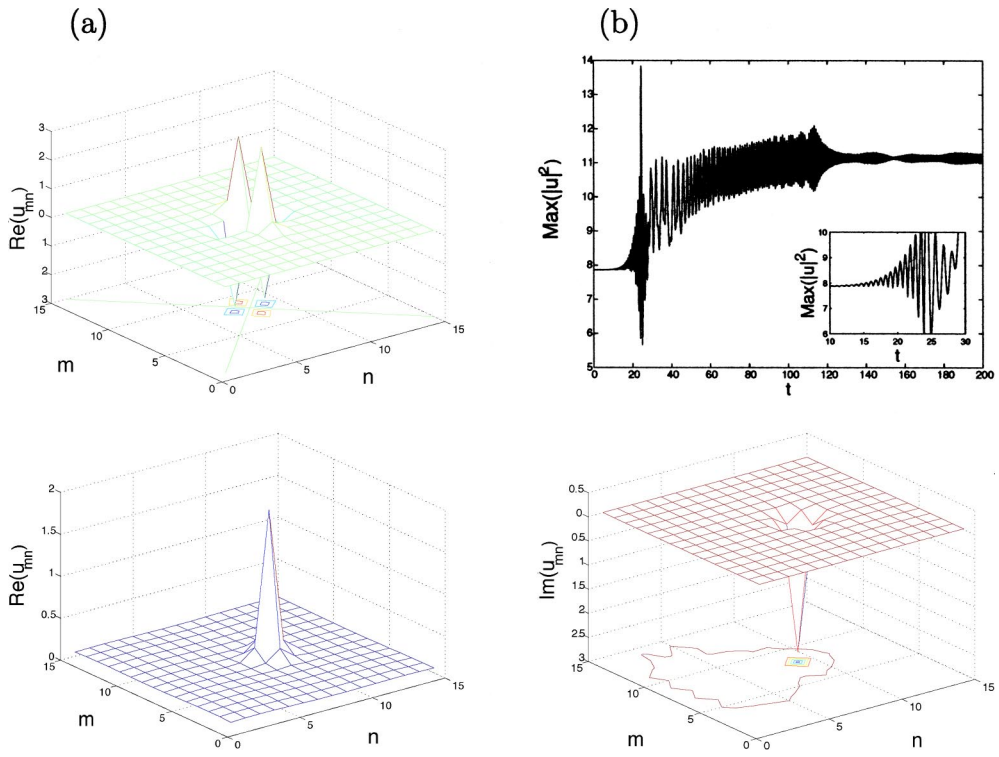

FIG. 4. (Color online) The top left panel shows the unstable quasivortex corresponding to $S=2$, in the case of $C=1$. The top right panel shows the oscillatory instability, setting in around $t=15$ in the evolution of the lattice field. The bottom panels show the real and imaginary parts of the established stable configuration (at $t=200$), which is identified as an ordinary stable zero-vorticity soliton.

bifurcation resulting from the collision of two imaginary eigenvalue pairs with opposite Krein signatures, which gives rise to a quartet of complex eigenvalues. The stability region is

$$C \leqslant C_{\mathrm{cr}}^{(2)} = 0.862 \tag{8}$$

[cf. the stability intervals (5) for $S=0$ and $S=1$ solitons, and the one (7) for $S=3$]. The profile of the solution generated by the real part initial ansatz (6), and the spectral plane of the stability eigenvalues associated with it, are displayed in a stable case, for $C=0.02$, in the middle panel, and at the instability onset, at $C=0.862$, in the bottom panel of Fig. 3. It is clear that the resulting solution follows a pattern of $\cos(2\theta)$ (for $S=2$) along the lattice.

Development of the instability of these solitons for $C>0.862$ was studied by direct simulations of Eq. (1). A typical example is shown in Fig. 4 for $C=1$: the oscillatory instability transforms the initial state into an ordinary zero-vorticity lattice soliton, which is a stable solution in this case.

The interpretation of solutions of this type in terms of the vorticity is ambiguous, as the solution is a purely real one. As is obvious from Fig. 3, the solution is actually a quadrupole localized on four lattice sites, with zeros between them, which is typical for vortex solutions that must vanish at the central point. The phase of the solution jumps by π when comparing positive and negative real values of the solution at adjacent sites carrying the solutions. To understand the global vorticity that may be ascribed to the solution, one can add a small perturbation which makes the solution complex and thus makes it possible to define a phase field across the lattice (this, obviously, corresponds to a situation expected in the experiment, where perturbations are inevitable). To this end, we tried perturbations based on all the localized eigenmodes of small perturbations around the stable stationary states of the present type. In Fig. 5, a full set of contour plots of eigenmodes is displayed for the same case (with $C=0.02$) which was used as an example in Fig. 3. The most essential peculiarity of the eigenmodes is that they are completely localized on the same set of four sites which carry the unperturbed solution.

Straightforward consideration demonstrates that a combination of the stationary solution and first eigenmode (the one with the eigenvalue $\lambda_1 \equiv i\omega_1 \approx 0.08i$), taken with a small amplitude, may give rise to the following phase distribution along a closed route connecting the four sites:

$$0 \to \pi \to 0 \to \pi \to 0, \tag{9}$$

or the same multiplied by (-1). In fact, the perturbed configuration oscillates, at the frequency ω_1, between these two phase patterns. Next, the second and third eigenmodes, which belong to the eigenvalue, $\lambda_{2,3} \equiv i\omega_{2,3} \approx 0.04i$, if added, with a small amplitude, to the unperturbed state, may give rise to phase patterns of the types

$$0 \to \pi \to 0 \to -\pi \to 0, \text{ or } 0 \to \pi \to 2\pi \to \pi \to 0 \tag{10}$$

(we take into account a possibility of a combination of the two latter eigenmodes). None of these patterns is character-

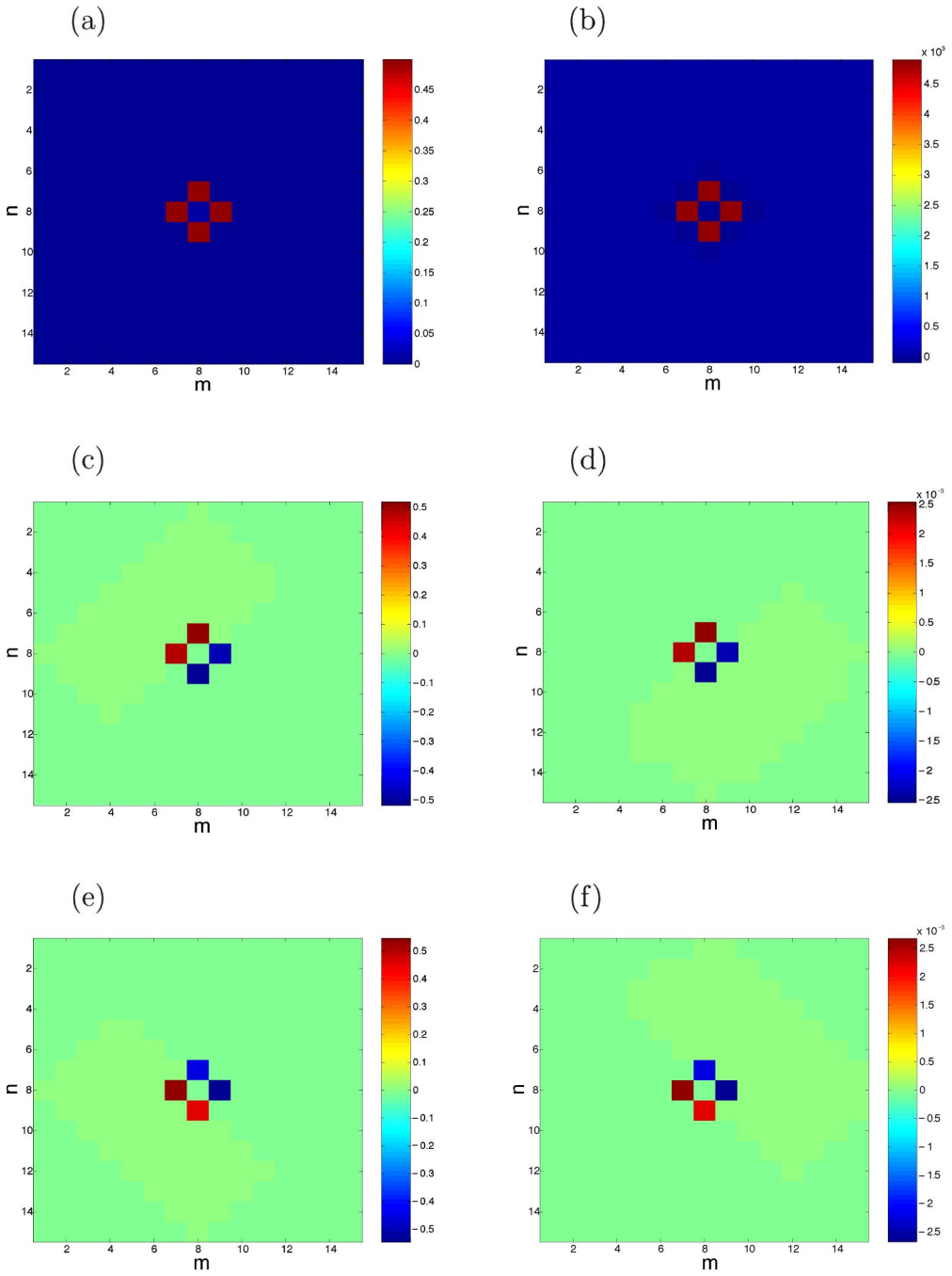

FIG. 5. (Color online) The panels display, in the form of contour plots, the real (left panels) and imaginary (right panels) parts of the full set of three localized eigenmodes of small perturbations around the stable quasivortex corresponding to the $S=2$ solution, in the case of $C=0.02$ (the same case as presented in Fig. 3). The first eigenmode (top panels) corresponds to the frequency $\omega_1 \approx 0.08$, and the two other eigenmodes (middle and bottom panels) belong to the frequency $\omega_{2,3} \approx 0.04$.

ized by a nonzero net phase gain generated by the round trip along the closed route, so the pattern cannot be ascribed finite vorticity. However, this is clearly a type of stable localized 2D lattice solutions drastically different from the ordinary zero-vorticity solitons. While this solution has no vorticity, it may be characterized by the largest intrinsic phase difference $(|\Delta\phi|)_{\max}$. This quantity is different from zero, but it depends on the way a small perturbation is added: $(|\Delta\phi|)_{\max}=\pi$ in the case of Eq. (9), and $(|\Delta\phi|)_{\max}=2\pi$ in the case of Eq. (10). We call this type of *real solution* a quasivortex.

We stress that *complex* localized solutions to the 2D DNLS equation, which are true vortices with $S=2$, were found in Ref. [23]. They were constructed starting with a complex ansatz, whose real and imaginary parts, unlike those in the expression (6), emulated the continuum model's expressions $\cos(2\theta)$ and $\sin(2\theta)$, where θ is the angular variable in the plane. However, it was found in Ref. [23] (and

rechecked in the course of the present work) that those true vortices are unstable through a real eigenvalue pair.

We have also constructed real quasivortices corresponding to $S=4$ [i.e., generated by the real part of the initial ansatz (6) with $S=4$]. These results will be reported in detail elsewhere. However, it is worth mentioning that their stability interval is [cf. Eqs. (8) and (7)] $C \leqslant C_{\mathrm{cr}}^{(4)}=0.292$. As expected from the comparison with known results for continuum models (with competing nonlinearities) [32,33], the stability interval shrinks (but does not disappear) with the increase of S, which equally pertains to the true vortices and quasivortices.

V. CONCLUSIONS

In this work, we have constructed solutions which are candidates for the role of stable higher-order localized vortices in the nonlinear dynamical lattice. The solutions generated by the initial ansatz with vorticity $S=3$ are true complex vortices, while the ones corresponding to $S=2$ and $S=4$ are purely real quasivortices, which actually present a different type of lattice solitons. For solutions of each type, the analysis of perturbation eigenmodes produces a stability interval, which shrinks with the increase of S (while true complex vortices with $S=2$, which were found in the earlier work [23], are unstable). The evolution of unstable states was investigated by means of direct simulations, with a conclusion that the unstable $S=3$ vortices split into a set of two separated stable solitons with $S=1$ and $S=0$, while the quasivortex corresponding to $S=2$ transforms itself into an ordinary zero-vorticity soliton.

These results are not only relevant to the general theory of dynamical lattices. They apply directly to bundled arrays of nonlinear optical waveguides and, indirectly (as the underlying nonlinearity is different), to waveguiding structures in the form of virtual lattices in photorefractive media. In these settings, the results suggest the possibility of existence of additional types of spatial optical solitons. In particular, the recent experimental demonstration of stable fundamental discrete vortices in 2D photonic lattices with self-focusing nonlinearity in Ref. [26] suggests that the higher-order vortices may be observed in the same medium. Experiments are currently under way with vortex masks corresponding to $S=3$ and $S=4$ [34]. Another direct application of the theoretical results reported in this paper is prediction of vortex and quasivortex solitons in BECs loaded in optical lattices, under realistic experimental conditions.

ACKNOWLEDGMENTS

P.G.K. gratefully acknowledges support from NSF Grant No. DMS-0204585 and the Eppley Foundation for Research. The work of B.A.M. was supported, in part, by Grant No. 8006/03 from the Israel Science Foundation. The work of Z.C. was supported by AFOSR, ARO, and NNSF of China.

[1] S. Aubry, Physica D **103**, 201 (1997); S. Flach and C. R. Willis, Phys. Rep. **295**, 181 (1998); Physica D **119** (1999), special issue edited by S. Flach and R. S. MacKay; Chaos **13**, 586 (2003); focus issue edited by Yu. S. Kivshar and S. Flach.

[2] A. A. Sukhorukov, Y. S. Kivshar, H. S. Eisenberg, and Y. Silberberg, IEEE J. Quantum Electron. **39**, 31 (2003); U. Peschel, R. Morandotti, J. M. Arnold, J. S. Aitchison, H. S. Eisenberg, Y. Silberberg, T. Pertsch, and F. Lederer, J. Opt. Soc. Am. B **19**, 2637 (2002).

[3] A. Trombettoni and A. Smerzi, Phys. Rev. Lett. **86**, 2353 (2001); F. Kh. Abdullaev, B. B. Baizakov, S. A. Darmanyan, V. V. Konotop, and M. Salerno, Phys. Rev. A **64**, 043606 (2001); F. S. Cataliotti, S. Burger, C. Fort, P. Maddaloni, F. Minardi, A. Trombettoni, A. Smerzi, and M. Inguscio, Science **293**, 843 (2001); A. Smerzi, A. Trombettoni, P. G. Kevrekidis, and A. R. Bishop, Phys. Rev. Lett. **89**, 170402 (2002); M. Greiner, O. Mandel, T. Esslinger, T. W. Hansch, and I. Bloch, Nature (London) **415**, 39 (2002); G. Kalosakas, K. Ø. Rasmussen, and A. R. Bishop, Phys. Rev. Lett. **89**, 030402 (2002).

[4] E. N. Pelinovsky and S. K. Shavratsky, Physica D **3**, 410 (1981).

[5] P. Binder, D. Abraimov, A. V. Ustinov, S. Flach, and Y. Zolotaryuk, Phys. Rev. Lett. **84**, 745 (2000); E. Trías, J. J. Mazo, and T. P. Orlando, *ibid.* **84**, 741 (2000).

[6] M. Peyrard, and A. R. Bishop, Phys. Rev. Lett. **62**, 2755 (1989); T. Dauxois, M. Peyrard, and A. R. Bishop, Phys. Rev. E **47**, R44 (1993); **47**, 684 (1993); M. Peyrard, T. Dauxois, H. Hoyet, and C. R. Willis, Physica D **68**, 104 (1993); A. Campa and A. Giansanti, Phys. Rev. E **58**, 3585 (1998).

[7] P. G. Kevrekidis, K. Ø. Rasmussen, and A. R. Bishop, Int. J. Mod. Phys. B **15**, 2833 (2001).

[8] D. N. Christodoulides and R. I. Joseph, Opt. Lett. **13**, 794 (1988); A. Aceves, C. De Angelis, G. G. Luther, and A. M. Rubenchik, *ibid.* **19**, 1186 (1994).

[9] H. Eisenberg, Y. Silberberg, R. Morandotti, A. R. Boyd, and J. S. Aitchison, Phys. Rev. Lett. **81**, 3383 (1998); R. Morandotti, U. Peschel, J. S. Aitchison, H. S. Eisenberg, and Y. Silberberg, *ibid.* **83**, 2726 (1999); H. S. Eisenberg, R. Morandotti, Y. Silberberg, J. M. Arnold, G. Pennelli, and J. S. Aitchison, J. Opt. Soc. Am. B **19**, 2938 (2002); J. Meier, J. Hudock, D. Christodoulides, G. Stegeman, Y. Silberberg, R. Morandotti, and J. S. Aitchison, Phys. Rev. Lett. **91**, 143907 (2003).

[10] D. Cheskis, S. Bar-Ad, R. Morandotti, J. S. Aitchison, H. S. Eisenberg, Y. Silberberg, and D. Ross, Phys. Rev. Lett. **91**, 223901 (2003).

[11] J. W. Fleischer, T. Carmon, M. Segev, N. K. Efremidis, and D. N. Christodoulides, Phys. Rev. Lett. **90**, 023902 (2003); J. W. Fleischer, M. Segev, N. K. Efremidis, and D. N. Christodoulides, Nature (London) **422**, 147 (2003).

[12] I. E. Papacharalampous, P. G. Kevrekidis, B. A. Malomed, and D. J. Frantzeskakis, Phys. Rev. E **68**, 046604 (2003).

[13] T. Pertsch, U. Peschel, F. Lederer, J. Burghoff, M. Will, S. Nolte, and A. Tunnermann, Opt. Lett. **29**, 468 (2004).

[14] G. L. Alfimov, P. G. Kevrekidis, V. V. Konotop, and M. Salerno, Phys. Rev. E **66**, 046608 (2002).
[15] N. K. Efremidis, S. Sears, D. N. Christodoulides, J. W. Fleischer, and M. Segev, Phys. Rev. E **66**, 046602 (2002).
[16] H. Martin, E. D. Eugenieva, Z. Chen, and D. N. Christodoulides, Phys. Rev. Lett. **92**, 123902 (2004).
[17] A. A. Sukhorukov, D. Neshev, W. Krolikowski, and Y. S. Kivshar, Phys. Rev. Lett. **92**, 093901 (2004).
[18] Z. Chen, H. Martin, E. D. Eugenieva, J. Xu, and A. Bezryadiua, Phys. Rev. Lett. **92**, 143902 (2004).
[19] D. Neshev, E. Ostrovskaya, Y. Kivshar, and W. Krolikowski, Opt. Lett. **28**, 710 (2003).
[20] S. Darmanyan, A. Kobyakov, and F. Lederer, JETP **86**, 682 (1998); P. G. Kevrekidis, A. R. Bishop, and K. Ø. Rasmussen, Phys. Rev. E **63**, 036603 (2001).
[21] P. G. Kevrekidis and V. V. Konotop, Phys. Rev. E **65**, 066614 (2002); M. Öster, M. Johansson, and A. Eriksson, *ibid.* **67**, 056606 (2003).
[22] P. G. Kevrekidis, B. A. Malomed, and Z. Musslimani, Eur. Phys. J. D **23**, 421 (2003); A. V. Gorbach and M. Johansson, Phys. Rev. E **67**, 066608 (2003).
[23] B. A. Malomed and P. G. Kevrekidis Phys. Rev. E **64**, 026601 (2001).
[24] P. G. Kevrekidis, B. A. Malomed, and A. R. Bishop, J. Phys. A **34**, 9615 (2001).
[25] T. Cretegny and S. Aubry, Phys. Rev. B **55**, R11929 (1997); M. Johansson, S. Aubry, Yu. B. Gaididei, P. L. Christiansen, and K. Ø. Rasmussen, Physica D **119**, 115 (1998).
[26] D. N. Neshev, T. J. Alexander, E. A. Ostrovskaya, Y. S. Kivshar, H. Martin, I. Makasyuk, and Z. Chen, Phys. Rev. Lett. **92**, 123903 (2004).
[27] J. W. Fleischer, G. Bartal, O. Cohen, O. Manela, M. Segev, J. Hudock, and D. N. Christodoulides, Phys. Rev. Lett. **92**, 123904 (2004).
[28] B. Baizakov, B. A. Malomed, and M. Salerno, Europhys. Lett. **63**, 642 (2003).
[29] J. Yang and Z. Musslimani, Opt. Lett. **23**, 2094 (2003).
[30] B. Baizakov, B. A. Malomed, and M. Salerno in *Nonlinear Waves: Classical and Quantum Aspects*, edited by F. Kh. Abdullaev and V. V. Konotop (Kluwer Academic, Dordrecht, 2004), p. 61; H. Sakaguchi and B. A. Malomed, J. Phys. B **37**, 2225 (2004); E. A. Ostrovskaya and Yu. J. Kivshar, Phys. Rev. Lett. **93**, 160405 (2004).
[31] L.-C. Crasovan, B. A. Malomed, and D. Mihalache, Pramana, J. Phys. **57**, 1041 (2001); B. A. Malomed, L.-C. Crasovan, and D. Mihalache, Physica D **161**, 187 (2002).
[32] R. L. Pego and H. A. Warchall, J. Nonlinear Sci. **12**, 347 (2002).
[33] D. Mihalache, D. Mazilu, B. A. Malomed, and F. Lederer, Phys. Rev. E **69**, 066614 (2004).
[34] J. Yang, I. Makasyuk, H. Martin, P. G. Kevrekidis, B. A. Malomed, D. J. Frantzeskakis, and Z. Chen (unpublished).
[35] M. Johansson and S. Aubry, Phys. Rev. E **61**, 5864 (2000).
[36] J.-C. van der Meer, Nonlinearity **3**, 1041 (1990).
[37] D. V. Skryabin, Phys. Rev. E **64**, 055601 (2001).
[38] T. Kapitula, P. G. Kevrekidis, and B. Sandstede, Physica D **193**, 263 (2004).